Thrombus Growth and Embolism on Tissue Factor-Bearing Collagen Surfaces Under Flow

Role of Thrombin With and Without Fibrin

Thomas V. Colace, Ryan W. Muthard, Scott L. Diamond

Objective—At sites of vascular injury, thrombin is an important mediator in thrombus growth and stability. Using microfluidic flow devices as well as patterned surfaces of collagen and tissue factor (TF), we sought to determine the role that fibrin plays in clot stability without interfering with the production of thrombin.

Methods and Results—We deployed an 8-channel microfluidic device to study coagulation during corn trypsin inhibitor–treated (XIIa-inhibited) whole blood perfusion over lipidated TF linked to a fibrillar collagen type 1 surface. Clot growth and embolization were measured at initial inlet venous (200 s^{-1}) or arterial (1000 s^{-1}) wall shear rates under constant flow rate or pressure relief mode in the presence or absence of Gly-Pro-Arg-Pro (GPRP) to block fibrin polymerization. Numerical calculations for each mode defined hemodynamic forces on the growing thrombi. In either mode at inlet venous flow, increasing amounts of TF on the surface led to a modest dose-dependent increase (up to 2-fold) in platelet deposition, but resulted in massive fibrin accumulation (>50-fold) only when exceeding a critical TF threshold. At a venous inlet flow, GPRP led to a slight 20% increase in platelet accumulation ($P<0.01$) in pressure relief mode with thrombi resisting ≈1500 s^{-1} before full channel occlusion. GPRP-treated thrombi were unstable under constant flow rate, where shear forces caused embolization at a maximum shear rate of ≈2300 s^{-1} (69 dynes/cm^2). In constant flow rate mode, the nonocclusive platelet-fibrin deposits (no GPRP) withstood maximum shear rates of ≈29 000 s^{-1} (870 dyne/cm^2) at ≈95% of full channel occlusion. For arterial inlet shear rate, embolization was marked for either mode with GPRP present when shear forces reached 87 dynes/cm^2 (≈2900 s^{-1}). Under constant flow rate, platelet-fibrin deposits (no GPRP) withstood maximums of 2400 dynes/cm^2 (80,000 s^{-1}) at ≈90% of full channel occlusion prior to embolization.

Conclusion—Fibrin increased clot strength by 12- to 28-fold. Under pressure relief mode, ≈2-fold more fibrin was produced under venous flow ($P<0.001$). These studies define embolization criteria for clots formed with surface TF-triggered thrombin production (±fibrin) under venous and arterial flows. **(*Arterioscler Thromb Vasc Biol*. 2012;32:1466-1476.)**

Key Words: arterial thrombosis ■ clot strength ■ coagulation ■ fibrin ■ thrombosis

Under hemodynamic conditions, blood coagulation on a damaged vessel is triggered by exposure of collagen and tissue factor (TF). A competition exists between the rate of platelet coverage of the damaged site and the ability of soluble factor X (FX) to access TF/FVIIa complex on the surface for local generation of FXa and, in turn, thrombin.[1–3] A second competition exists between the ability of thrombin to activate platelets, its ability to activate fibrinogen, its consumption by incorporation into fibrin, and its rapid dilution downstream under flow conditions.[4–6] A third competition exists between flow delivering platelets to the clotting event (both by direct axial convection and red blood cell–mediated radial transport) and shearing forces that remove individual platelets or cause large-scale embolism. Furthermore, at pathological shear rates above ≈5000 s^{-1}, von Willebrand Factor can undergo conformational changes, and shear stress can activate platelets.[7,8] The interplay between these competitions under flow, in concert with blood and wound characteristics, dictates how rapidly a clot grows, its composition, its propensity to embolize, and the likelihood of occlusion. For example, basic questions about why severe hemophiliacs bleed (while afibrinogenemia patients do not) include subtleties about whether the bleeding defect is due to poor platelet activation, poor fibrin polymerization, low TF levels in mechanically stressed joints, or a combination of these deficits.

Although platelet deposition and local thrombin production under flow are distinct but intertwined processes in human disease and animal injury models,[9,10] they are often studied independently in vitro due to the difficulty of creating a collagen surface that is procoagulant via extrinsic tenase, TF/FVIIa. In a recent study, we demonstrated the linkage of lipidated TF to collagen surfaces in a microfluidic model of vessel injury.[11]

Received on: January 30, 2012; final version accepted on: April 10, 2012.

From the Department of Chemical and Biomolecular Engineering, Institute for Medicine and Engineering, University of Pennsylvania, Philadelphia, PA.

The online-only Data Supplement is available with this article at http://atvb.ahajournals.org/lookup/suppl/doi:10.1161/ATVBAHA.112.249789/-/DC1.

Correspondence to Dr Scott L. Diamond, Department of Chemical and Biomolecular Engineering, Institute for Medicine and Engineering, 1024 Vagelos Research Laboratories, University of Pennsylvania, Philadelphia, PA 19104. E-mail sld@seas.upenn.edu

This approach extends earlier studies that use supported TF bilayers without collagen[12,13] or simply mixed lipidated TF onto collagen surfaces.[5] Distinct from studies that add TF to blood before perfusion over collagen or allow the contact pathway to generate thrombin throughout the weakly anticoagulated blood,[14] the presentation of both TF and collagen on a surface allows the combined study of platelet deposition in combination with local thrombin generation akin to the in vivo laser injury model.[15,16] In the present study, we use the same techniques, but take advantage of the ability to control the hemodynamic conditions experienced at the thrombotic injury site. We have developed 2 distinct modes of whole blood perfusion: constant flow rate and pressure relief mode. Perfusion of blood at constant flow rate through a microfluidic device or flow chamber allows a precisely controlled experiment, however thrombotic occlusion is not possible because the clot cannot stop a syringe pump. In this mode, growing platelet masses experience a constant flow rate, but are subjected to increasingly large wall shear rates as they begin to occlude the containing channel. In a second and more physiologically (and pathophysiologically) relevant mode of operation, pressure relief mode, flow is diverted from thrombotic occluding channels to open channels which then allows a thrombus to grow to a full occlusion. In this mode, shear stresses increase as flow squeezes past the growing thrombus, however once the thrombus blocks $>\approx 80$ % of the flow path, a large pressure drop (ie, flow resistance) exists to divert flow to the open channel, and shear forces decrease, eventually to zero at full occlusion. These 2 modes of operation, in combination with computational fluid dynamics simulations of flow during device operation, have allowed us to investigate the stability of growing clots and the effects of surface TF levels on platelet adhesion and fibrin production. Furthermore, the use of Gly-Pro-Arg-Pro (GPRP) to block fibrin polymerization allowed a determination of thrombin effects on clot growth and stability, independent of fibrin formation. Fibrin results in clots that are up to 28× stronger than platelet deposits, and can resist shear stresses up to ≈2400 dyne/cm^2 when the platelet-fibrin thrombus is exposed to arterial flows reaching wall shear rates of 80 000 s^{-1}. For surface presentation of TF and collagen, a sharp threshold concentration exists that was needed to trigger fibrin production which is in excess of that needed to enhance platelet deposition. Also, surface presentation of TF and collagen results in a mixture of aggregated platelets and fibrin which is more platelet-rich at the front of the thrombus and more fibrin-rich at the tail end, consistent with simulation of thrombin flux from a thrombus surface.

Materials and Methods

Sample Collection and Preparation

Blood was collected through venipuncture from a group of 8 healthy men (aged 22–28 years) who had refrained from taking oral medication for at least 10 days, and were self-reported as free from disease and any bleeding disorders. All samples were collected in accordance with the University of Pennsylvania Internal Review Board, and all donors had provided informed consent. Samples were drawn into a final concentration of 40-μg/mL corn trypsin inhibitor (CTI, Haematologic Technologies, Essex Junction, VT) to inhibit coagulation by the contact pathway. All samples were treated with anti-CD61 (clone VI-PL2) fluorescently conjugated antibody (Becton Dickinson, Franklin Lakes, NJ; 0.125-μg/mL final concentration) and a fluorescently conjugated fibrin-specific antibody[17,18] (T2G1, gift from the Mortimer Poncz laboratory, Children's Hospital of Philadelphia; 0.5-μg/mL final concentration). Although clone T2G1 does interfere with the fibrin B:b interaction, this had no effect on fibrin polymerization in this assay (Figure I in the online-only Data Supplement). Immediately before perfusion, samples were treated with GPRP (Sigma, St. Louis, MO; 5-mmol/L final concentration) in HEPES-buffered saline (20-mmol/L HEPES, 150-mmol/L NaCl, pH 7.4). All samples were used within 10 minutes of phlebotomy.

Relipidation of TF Into Vesicles and Linking to Collagen Surfaces

Recombinant TF (American Diagnostica Inc, Stamford, CT) was incorporated into liposomes in a 1:10 000 protein to lipid ratio as previously described.[19] Briefly, liposomes consisting of 79% phosphatidylcholine, 20% phosphatidylserine, and 1% biotinylated phosphatidylethanolamine (Avanti Polar Lipids, Alabaster, AL) were generated after a protocol by Smith et al. The liposomes were treated with 4-mmol/L Triton X-100 (Sigma) before addition of the TF to allow incorporation into the membrane with gentle mixing. The detergent was removed using Bio-Beads SM-2 (BioRad, Hercules, CA). The final TF-liposomes were stored at −80°C until use.

Surfaces of acid-insoluble equine type 1 collagen fibrils (Chrono-Par, Chrono-Log, Havertown, PA) were formed in single microfluidic channels 250 μm by 1 cm in length on glass briefly treated with Sigmacote (Sigma) to create a hydrophobic substrate. The collagen solution (1 mg/mL) was allowed to rest on the glass surface for 30 minutes before the channel was washed with 0.5% bovine serum albumin (BSA) in HEPES-buffered saline. The channel was then perfused with a biotinylated polyclonal antibody against collagen type 1 (40 μg/mL; Abcam, Cambridge, MA), and allowed to rest for 5 minutes before another wash with BSA. Immediately thereafter, the channel was filled with streptavidin (100 μg/mL; Sigma), and allowed to rest for 5 minutes before rinsing with BSA. Finally, the channels were filled with undiluted TF-liposomes or TF-liposomes diluted with empty liposomes and allowed to incubate for 1 hour. The channels were rinsed with BSA, the patterning device removed, and the 8-lane flow devices were affixed perpendicular to the patterned protein strip. The flow devices were filled with BSA a minimum of 30 minutes before perfusion with whole blood to prevent nonspecific interactions with glass or poly(dimethylsiloxane). Smith et al[19] demonstrated that recovery of TF into the liposomes using the previously described preparation is near complete and that 50% of imbedded molecules are exposed to the bulk. Therefore, we estimate 10 molecules of TF per liposome are presented to the flow. If a tightly packed monolayer of liposomes were achieved on the surface, an upper limit would be ≈100 molecules TF/μm^2. Because liposomes were confined to the collagen fibers on the surface, a more accurate estimation based on imaging of ≈10% surface coverage is ≈10 molecules TF/μm^2.

Fabrication of Microfluidic Devices and Real-Time Imaging

The microfluidic devices, described by Maloney et al,[20] consisted of 8 parallel channels 250 μm wide by 60 μm tall generated in poly(dimethylsiloxane) (Sylgard, Ellsworth Adhesives, Germantown, WI). The device was fed by 8 separate inlets, with perfusion achieved by withdrawal into a syringe pump (Harvard Apparatus, Holliston, MA) from 1 common outlet. Approximately 1 cm from the inlet, the channels were spaced close enough to allow all 8 channels to be imaged simultaneously in a single 2× field of view using an inverted microscope (IX81, Olympus America, Center Valley, PA) equipped with a charge-coupled device (Hamamatsu, Bridgewater, NJ). A custom stage insert held 3 microfluidic devices allowing 24 simultaneous clotting events to be imaged in 24-second intervals (Figure II in the online-only Data Supplement).

Perfusion Experiments

All experiments were run in 1 of 2 different flow modes. First, constant flow rate experiments were conducted such that each of the 8 available channels was perfused with the same sample of whole blood from a single donor. This ensured that platelet adhesion at the model injury site was comparable between all lanes, such that differences in flow rates between channels would not exist. When devices were perfused under pressure relief mode, every other channel was fed with whole blood treated with 5-mmol/L EDTA (Sigma) to chelate calcium and ablate platelet adhesion. This led to an increase in flow in EDTA-treated channels because platelets obstructed untreated lanes.

Each flow mode was run at a venous or arterial initial wall shear rate (200 or 1000 s^{-1}) and in the presence or absence of 5-mmol/L GPRP to block fibrin polymerization during thrombin generation. This resulted in a set of 8 experimental conditions which were run with a minimum of 3 unique donors, providing at least 12 clotting events under pressure relief mode or 24 under constant flow rate. Interdonor, as well as intradonor variability, was calculated by comparing platelet fluorescent intensity at the 432-second time point or the first time point before embolus and was $<$20% under venous shear rate conditions and $<$25% under arterial shear rate conditions (data not shown). For statistical purposes, all individual clotting events for a given set of flow conditions were considered. Statistical significance was calculated using the Student *t* test.

Determination of Clot Morphology and Confocal Imaging

Real-time clot height was determined by platelet fluorescent intensity, which was linearly proportional to the fluorescent intensity of a fully occluded thrombus (30 000$\pm$2000 AU). When conditions did not lead to embolus, final clot height was determined at the end of the experiment, if embolus did occur, the previous time point determined the final clot height. Profiles of clot morphology were generated using a custom MATLAB script, in which the average of 50 line scans (in the direction of flow) for 5 different clots were considered. The height at each location along the scan was also assumed to be proportional to the fluorescent intensity of a fully occluded thrombus.

Optical sectioning was performed in 2-μm increments with a disk spinning unit (IX2, Olympus America) over the 60-μm channel height immediately after cessation of flow. A 3-dimensional reconstruction of these images was created with the ImageJ software package (National Institutes of Health). Cross sections of this image were generated using a custom MATLAB script (MathWorks, Natick, MA).

Two-Dimensional and 3-Dimensional Computational Fluid Dynamics

A model microfluidic device consisting of 2 channels with separate inlets and a single outlet was generated in COMSOL Inc (Burlington, MA). The local wall shear rate was calculated to be 194 s^{-1} in an unobstructed, 60-μm tall channel with a flow rate of 2 μL/min. A thrombus was modeled in 1 of the channels by a 250-μm long trapezoidal cut out to mimic the shape and size of the growing thrombus. The conditions were considered constant flow rate when the flow rate at each of the inlets was set to 2 μL/min. The conditions were considered pressure relief mode when the flow rate at the outlet was set to 4 μL/min and the inlets were held at constant pressure.

Additionally, a 3-dimensional geometric model was created in COMSOL using parametric surface data from experimental platelet deposition. Due to computational limitations, intricate surface features were averaged to produce a model with surface resolution of 1.91 μm^2/pixel. Thrombin concentrations and shear rates were modeled by imposing a thrombin flux[2] of 10 to 12 nmol/μm^2 s under constant 2-μL/min flow conditions.[21] The flux was assumed to be constant over the entire modeled platelet surface, and the resulting thrombin boundary layer was governed by convective and diffusive transport with a thrombin diffusion coefficient in water of 4.2×10^{-11} m^2/s.[21] Although the thrombus is porous and complex reaction dynamics regulate thrombin production, the model of a solid surface thrombus does account for the fact that thrombin is soluble and is ultimately released from the outer surface of the thrombus. We assume a constant thrombin release rate which corresponds to a pseudo steady-state assumption, a reasonable approach because thrombin release dynamics change on a time scale of many seconds and minutes, but the concentration boundary layer changes with subsecond dynamics.

Results

TF-Liposomes Potentiate Platelet Adhesion and Fibrin Deposition Under Flow

TF embedded in phosphatidylserine:phosphatidylcholine:biotinylated phosphatidylethanolamine liposomes was immobilized on a fibrillar type 1 collagen surface with a biotinylated antibody against collagen and streptavidin. The amount of TF presented to the flow could be controlled through the use of empty liposomes (phosphatidylserine:phosphatidylcholine:biotinylated phosphatidylethanolamine) to dilute the TF-bearing vesicles. Figure 1 demonstrates the effect of undiluted, 10-fold diluted, and 100-fold diluted TF-liposomes on platelet adhesion and fibrin deposition under 2 flow conditions: constant flow rate and pressure relief mode at an inlet venous shear rate of 200 s^{-1}. The results demonstrate a dilution-dependent reduction in both platelet adhesion and fibrin deposition under both conditions. No detectable fibrin was generated at 100-fold dilution of TF-liposomes and barely detectable levels of fibrin at 10-fold dilution. However, a dose-dependent increase in platelet deposition was observed with increasing surface TF, indicating that thrombin generation was still occurring at a concentration sufficient to activate platelets but insufficient to polymerize fibrin. Consistent with earlier studies with unlinked lipidated TF coincubated with surface collagen,[5] a strong threshold was observed between no fibrin and abundant

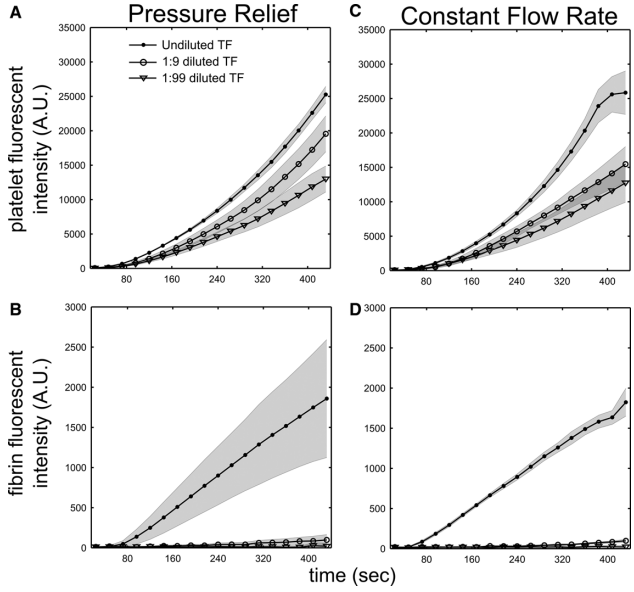

Figure 1. Whole blood corn trypsin inhibitor (CTI 40 μg/mL) was perfused at 200 s^{-1} over collagen surfaces with immobilized tissue factor (TF) that was undiluted or diluted 1:9 and 1:99 with empty liposomes. **A** and **B**, Platelet aggregation and fibrin production were measured with pressure relief (n=4) and at constant flow rate (**C** and **D**; n=8) in the absence of Gly-Pro-Arg-Pro (GPRP) and are presented$\pm$SD (shaded regions). Platelet accumulation decreased with increasing dilution of TF under both conditions. Fibrin production was also reduced after the first dilution in both flow environments, and was undetectable at 1:99 TF:empty liposomes.

fibrin when TF was elevated over a single decade of concentration from ≈1 to 10 TF molecules/μm². We observed that the increase in platelet deposition between undiluted and 10-fold diluted TF is >2-fold under constant flow rate. This may be explained by high shears (>5000 s^{-1}) experienced in this flow environment as full channel occlusion is approached. When run with pressure relief, excessive shear is avoided by the diversion of flow to empty channels. Similar trends were observed when the TF dilution was run at the arterial initial wall shear rate of 1000 s^{-1} (Figure III in the online-only Data Supplement).

Simulation of Local Flow Environments

The COMSOL multiphysics package was used to calculate the flow conditions in a 2-channel model of our microfluidic flow device. The 2-dimensional simulation mimics a vertical cross section (60 μm height) along the centerline of a pair of channels with independent inlets and a single outlet (Figure 2A). An inlet flow rates of 2 μL/min of whole blood (viscosity 3 cP) generated a wall shear rate of 194 s^{-1} and a pressure drop of 0.83 mm Hg in an empty channel, in agreement with our prior work.[22] A growing thrombus in 1 of the channels was represented by a 250-μm long trapezoidal cut out of varying heights. This length was chosen to mimic the size of the thrombi which form in the assay.

The pressure relief condition was replicated by setting the channel inlets to maintain a constant pressure and the outlet to maintain a constant flow rate (4 μL/min). Because the height of the occlusion was varied, a biphasic response in shear rate was calculated (Figure 2B). The maximum shear rate was >≈7-fold the starting shear rate, and this occurred at an occlusion of 80%, where flow rate was estimated to drop most rapidly as progression to full occlusion occurred (Figure 2C). Over the full range of vessel occlusion, the pressure drop across the device rose only 2-fold (1.66 mm Hg, Figure 2D), which is predicted by the 2-fold increase in flow rate in the unobstructed channel. Compared with the constant flow rate conditions where pressures increased by >150 mm Hg, pressure relief mode had <1-mm Hg increase as the channel approached full occlusion.

Flow conditions in constant flow rate mode corresponded to inlet flow rates of 2 μL/min and a constant pressure outlet. Figure 2E demonstrates that wall shear rates are monotonically increasing with increasing occlusion height. At an occlusion of

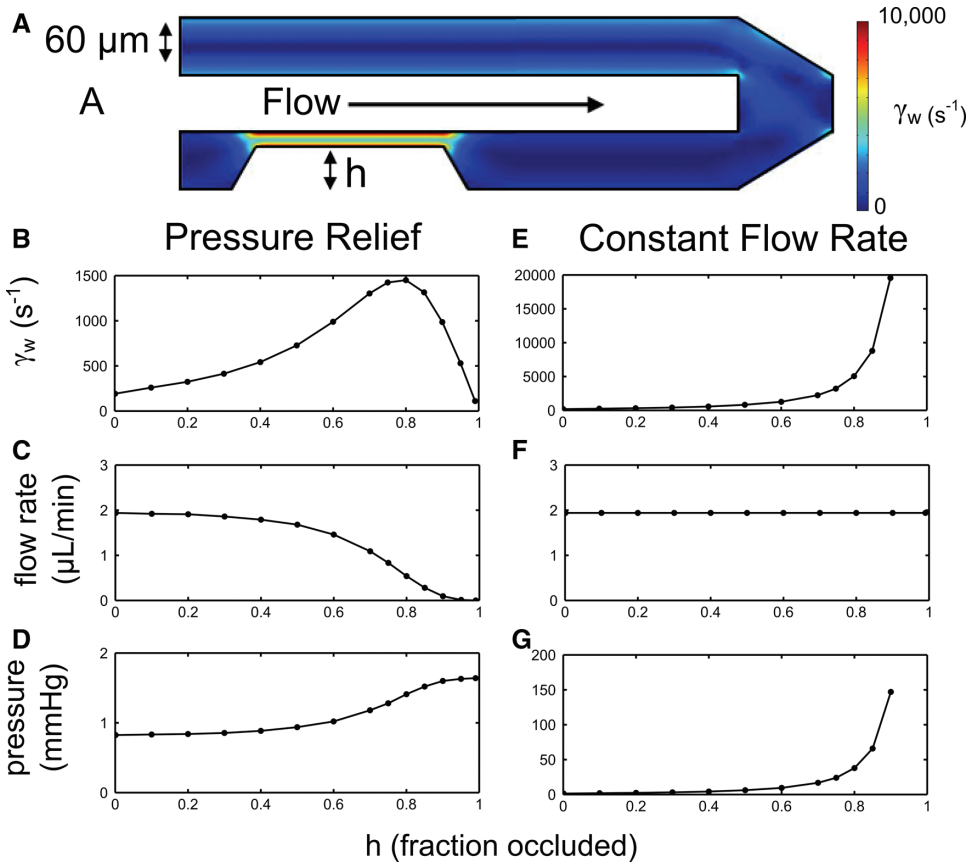

Figure 2. **A**, Flow through a vertical cross section of a pair of channels from the microfluidic device was modeled using COMSOL (the colors indicate local wall shear rate). The growing thrombus, with a variable height (h), was represented by a trapezoidal cut out in 1 of the channels. Two conditions were considered. **A** to **C**, Pressure relief mode was reproduced by defining the flow rate at the outlet to be 4 μL/min. The shear rate and flow rate were calculated at the wall in the center of the model thrombus and the pressure drop was measured across the device. The model demonstrates that the wall shear rate under these conditions increases until 80% occlusion, and then decreases as full channel occlusion is approached. Flow through the occluded channel begins to significantly decrease after 50% occlusion as the pressure drop increases 2-fold due to the diversion of flow into half of the original channel volume. **D** to **F**, Constant flow rate was specified by defining the inlet flow rate in each channel to be 2 μL/min. The simulation indicates that the wall shear rate rapidly increases when the occlusion reaches 70% of the channel height with a similar trend in the pressure drop.

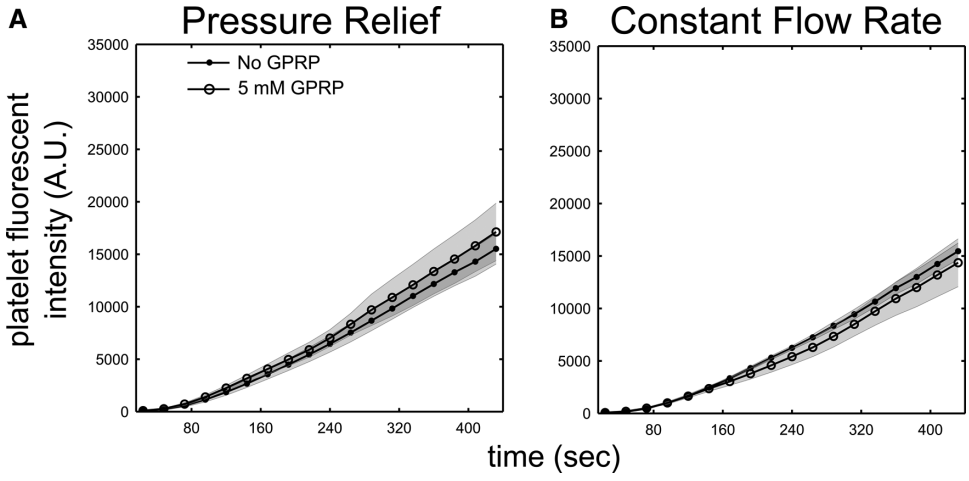

Figure 3. Whole blood treated with corn trypsin inhibitor (CTI 40 μg/mL) was perfused over fibrillar collagen surfaces in the absence of tissue factor–liposomes with pressure relief (**A**, n=4) or at constant flow rate (**B**, n=8) at an initial wall shear rate of 200 s^{-1}. Platelet adhesion to the collagen patch as well as fibrin deposition was measured simultaneously through the use of fluorescently conjugated antibodies. Platelet fluorescent intensity is presented±SD (shaded gray regions). No fibrin was detected under either flow condition. The addition of 5-mmol/L Gly-Pro-Arg-Pro (GPRP) to block fibrin polymerization (open circles) had no effect on the rate or final extent of platelet accumulation. Furthermore, the flow conditions also had no effect on platelet adhesion in these assays because the indicated fluorescent intensities represent ≈50% channel occlusion, which results in minimal changes in the hemodynamic conditions experienced by the growing platelet masses.

≈99%, shear rates were predicted to reach 2×10^6 s^{-1}. These rises are accompanied by increases in pressure drop across the channel with a similar trend (Figure 2G).

GPRP Does Not Affect Platelet Aggregation in the Absence of TF

GPRP, a tetrapeptide sequence known to interrupt the polymerization of fibrin, was used extensively in the present study to decouple the effects of thrombin and fibrin on platelet deposition and clot stability. As a control experiment, whole blood from a single donor (CTI 40 μg/mL) was perfused at a venous inlet shear rate (200 s^{-1}) over collagen surfaces lacking TF under pressure relief and constant flow rate in the presence and absence of 5-mmol/L GPRP. Platelet adhesion and fibrin deposition were measured over a 430-second perfusion, and were similar in the presence or absence of GPRP (Figure 3). No detectable fibrin was generated under any condition (data not shown), consistent with the lack of any kinetically significant blood-borne TF over the time frame of a 430-second clotting event on collagen (in the presence of CTI).

Effects of Flow Conditions and GPRP on Platelet Deposition and Fibrin Under Venous Flow

Whole blood (CTI 40 μg/mL) was perfused over TF/collagen surfaces at 200 s^{-1} to mimic venous flow conditions. Platelet deposition and fibrin deposition were measured in 24-second intervals in the presence and absence of 5-mmol/L GPRP. The height of the thrombus was calculated by assuming a linearly proportional relationship in platelet fluorescent intensity. The average platelet fluorescent intensity of multiple fully occluding thrombi was measured to be 30 000±2000 AU. The estimates of wall shear rate and flow rate based on these occlusions were calculated using the COMSOL computational fluid dynamics data (Figure 2).

Under pressure relief, the average platelet mass formed in the presence of GPRP included 20% more platelets than that formed without GPRP ($P<0.01$, Figure IVA in the online-only Data Supplement), suggesting a modest role for fibrin in slowing platelet deposition and clot growth. The aggregates formed under GPRP conditions consistently progressed to full occlusion under pressure relief conditions, and reached maximum shears of ≈1500 s^{-1}. Control clots (no GPRP) had yet to fully occlude at the end of the 430-second perfusion, possibly due to competition by fibrin generation. Movie I in the online-only Data Supplement demonstrates the morphological differences between clots grown on collagen+TF in the presence or absence of GPRP at venous flow conditions.

Under constant flow rate (Figure 4, right), GPRP and control clots appeared to grow at a similar rate for the first 240 seconds of perfusion. This is expected when channel occlusion is <50%, because conditions in each of the flow modes are similar. A 50% blockage results in minimal pressure drop as blood moves over the growing clot. The rate of growth of the platelet mass after 240 seconds appears slightly increased in the presence of GPRP, possibly due to competition by fibrin in the absence of GPRP. By 320 seconds, however, GPRP-treated clots embolized. The calculated average shear rate, obtained using the average height of the clots before first embolus was observed, was ≈1500 s^{-1} (45 dyne/cm^2). The maximum shear rate under these conditions calculated at the platelet fluorescent intensity corresponding to 1 SD above the mean fluorescence was 2300 s^{-1} (69 dyne/cm^2). Control clots with fibrin (no GPRP) appeared stable up to 29 000 s^{-1} (mean+SD; 870 dyne/cm^2) under these conditions but began to tear from the surface shortly after the 432-second time point (data not shown). The average platelet fluorescent intensity at the end of the experiment (or first embolization) was >≈40% ($P<0.001$; Figure IVB in the online-only Data Supplement) in the absence of GPRP. These results suggest at least a 12-fold increase in clot stability (ie, 870 versus 69 dyne/cm^2) attributable to fibrin. Also less fibrin was generated under the constant flow rate conditions compared with the pressure relief conditions ($P<0.001$; Figure V in the online-only Data Supplement), which may be explained by the higher shear rates experienced by the constant flow rate environment which would remove thrombin, fibrin monomer, and small multimers to a greater extent.

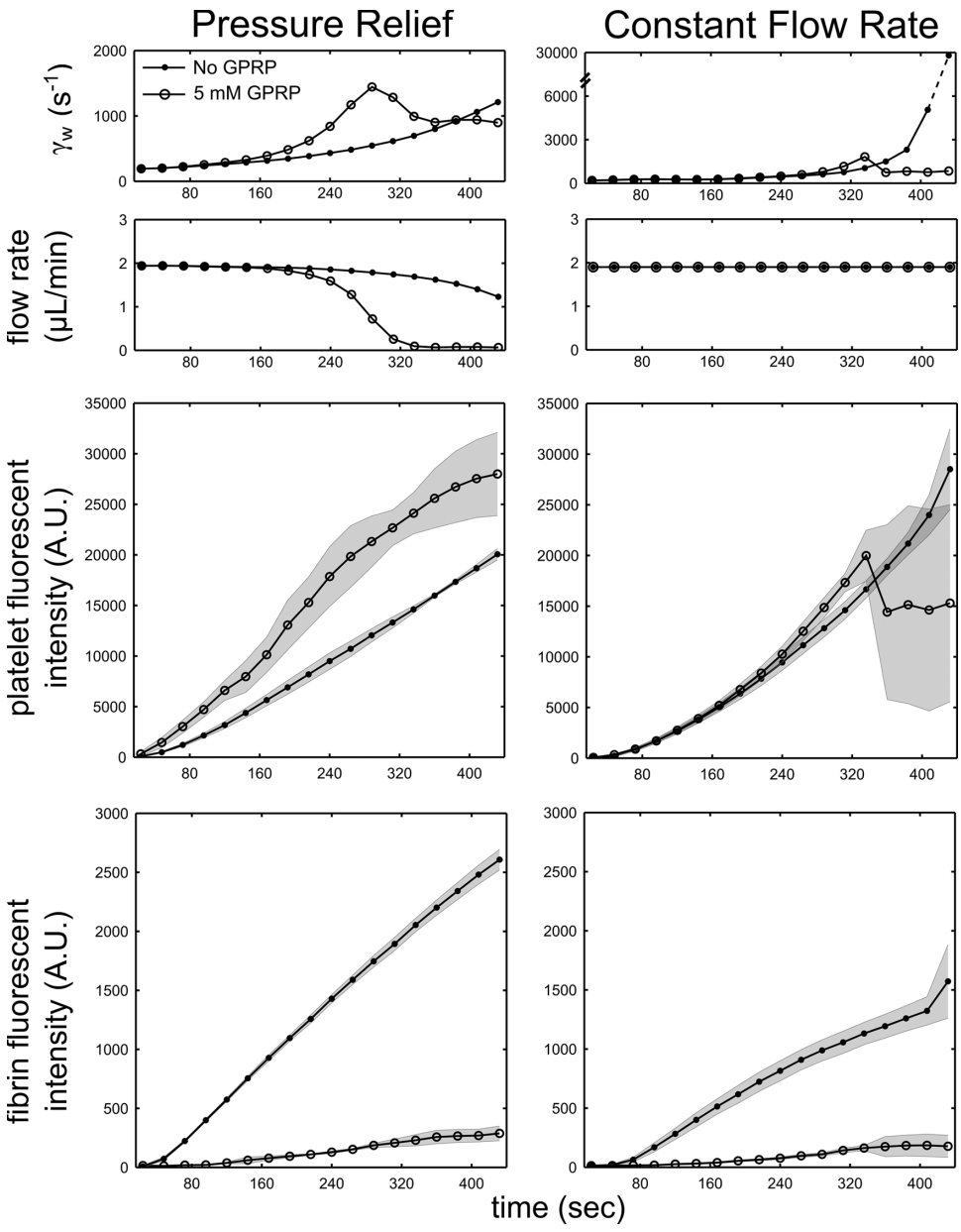

Figure 4. Whole blood corn trypsin inhibitor (CTI 40 μg/mL) in the presence or absence of 5-mmol/L Gly-Pro-Arg-Pro (GPRP) was perfused over a fibrillar collagen surface at an initial venous wall shear rate of 200 s^{-1}, with (left, n=4) or without (right, n=8) pressure relief. The data for each flow mode were collected in a single day from a single donor. They are representative of multiple experiments per condition. Platelet accumulation data were used to calculate the hemodynamic conditions at the thrombus boundary based on the simulation data. The platelet and fibrin accumulation at the collagen patch was measured in 24-second intervals for 430 seconds, and are presented±SD (shaded gray regions). Fibrin-free platelet deposits formed in the presence of GPRP were stable up to 2300 s^{-1} (shear stress of 69 dyn/cm^2) whereas thrombi with fibrin were stable up to 29 000 s^{-1} (870 dyn/cm^2) when formed at constant flow rate.

Effects of Flow Conditions and GPRP on Platelet Deposition and Fibrin Under Arterial Flow

Whole blood (CTI 40 μg/mL) was perfused over TF/collagen surfaces at 1000 s^{-1} to mimic arterial flow conditions. As before, platelet deposition and fibrin deposition were measured in 24-second intervals in the presence and absence of 5-mmol/L GPRP. In the arterial flow environment, control blood was unimpeded in the formation of fully occlusive thrombi in pressure relief mode (Figure 5, left). These platelet-fibrin thrombi formed more rapidly than under venous conditions, but had a 2-fold reduction in fibrin compared with venous flow conditions ($P<0.001$; Figure V in the online-only Data Supplement). At 80% of full channel occlusion, shear rates reached a maximum value of ≈7000 s^{-1} under these flow conditions. When samples were treated with GPRP to block fibrin polymerization, both embolization (n=4 devices) and full occlusion (n=2 devices) were observed. The average shear rate causing embolus under these conditions was ≈3100 s^{-1} (93 dyne/cm^2) and maximum shears of 5300 s^{-1} were sustained (159 dyne/cm^2). Figure IVA in the online-only Data Supplement demonstrates a significant ($P<0.001$) reduction in platelet accumulation (2-fold) between control clots and those treated with GPRP, when embolus occurred.

Under constant flow rate (Figure 5, right), platelet deposits grew rapidly and at similar rates for the first 120 to 140 seconds of perfusion in the presence and absence of GPRP. Platelets treated with GPRP were embolized at an average of 33% of full channel occlusion corresponding to 2300 s^{-1} (69 s^{-1}) whereas maximum sustained shear rates were calculated at 2900 s^{-1} (87 s^{-1}). Control platelet-fibrin clots were able to withstand an average 76% occlusion before embolus at a calculated shear rate of 17 000 s^{-1} (510 dyne/cm^2). Maximum shear rates sustained by control clots under arterial flow conditions were 83 000 s^{-1} (2490 dyne/cm^2) which corresponded to 90% channel occlusion.

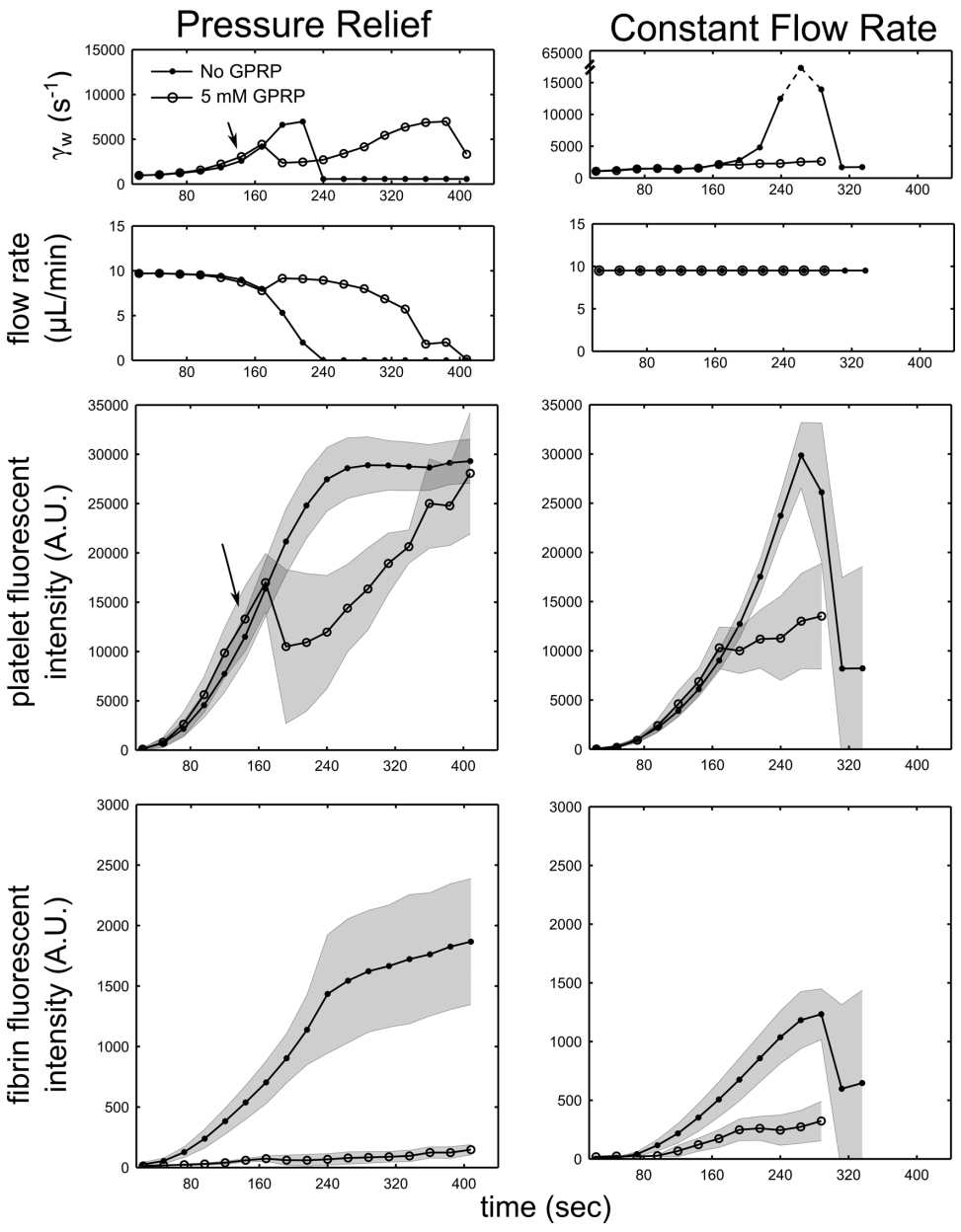

Figure 5. Whole blood corn trypsin inhibitor (CTI 40 μg/mL) in the presence or absence of 5-mmol/L Gly-Pro-Arg-Pro (GPRP) was perfused over a fibrillar collagen surface at an initial arterial wall shear rate of 1000 s^{-1}, with (left, n=4) or without (right, n=8) pressure relief. The data for each flow mode were collected in a single day from a single donor. They are representative of multiple experiments per condition. Platelet accumulation data were used to calculate the hemodynamic conditions at the thrombus boundary based on the simulation data. The platelet and fibrin accumulation at the collagen patch was measured in 24-second intervals for 430 seconds and are presented±SD (shaded gray regions). Under both flow conditions, platelet deposits formed in the presence of GPRP embolized before the end of the experiment. In the pressure relief case, the arrow indicates where the clots gave way to the flow and reorganized, at the 192-second time point, the clots begin to embolize, which appeared as a decrease in fluorescent intensity. Fibrin-rich clots provided stability up to 80 000 s^{-1} at constant flow rate conditions, and allowed for full occlusion under pressure relief conditions.

These data represent a 28-fold increase in clot stability (ie, 2490 versus 87 dyne/cm^2) attributable to the fibrin. Figure IVB in the online-only Data Supplement illustrates the significant reduction in platelets (135%; $P<0.001$) under these conditions±GPRP. Movie II in the online-only Data Supplement demonstrates the growth and embolization of 8 clots grown simultaneously in the presence of GPRP under arterial flow conditions.

Morphology of In Vitro Thrombi From Wall-Attached TF

Fluorescent micrographs of thrombus formation over time are presented in Figure 6 (platelets, green; fibrin, red). Initial platelet adhesion events occurred evenly over the 250×250-μm patch whereas early fibrin events emerge downstream. Later in thrombus development, platelet adhesion appears to concentrate at the upstream edge whereas fibrin was most intense downstream.

Profiles of clot height were generated by averaging line scans of fluorescent intensity drawn in the direction of flow over the 250-μm patch for several clots forming at an initial wall shear rate of 200 s^{-1} that were nonocclusive at various time points (Figure 7). These figures illustrate that, in the absence of TF (Figure 7A), platelet aggregates grew evenly over the collagen patch (denoted by vertical lines). When TF was added, however, platelet aggregates favored the upstream end of the collagen patch even growing beyond its borders (Figure 7B). Fibrin deposition was higher at the downstream edge of the collagen patch (Figure 7C). Heights of the fibrin mesh were determined by confocal microscopy. Under arterial inlet shear rate conditions, platelet accumulation was drastically decreased in the absence of TF (Figure 7D). These results are consistent with previous work[23] demonstrating a reduction of platelet accumulation at the inlet of a parallel plate flow chamber (<2-mm axial distance) between shear

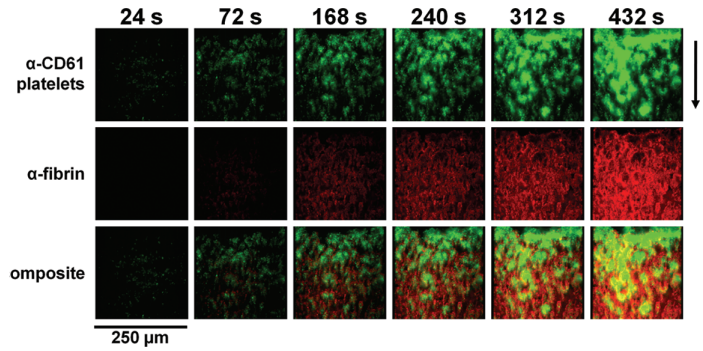

Figure 6. Whole blood corn trypsin inhibitor (CTI 40 μg/mL) was perfused over a collagen surface (200 s^{-1}; constant flow rate) under pressure relief conditions in the presence of fluorescently conjugated antibodies against platelet CD61 and fibrin. Flow is from top to bottom. The images demonstrate the growth of the platelet mass (top), the growth of the fibrin mesh (middle), and their composite (bottom) with perfusion time.

rates of 100 s^{-1} and 1500 s^{-1}. In the presence of TF, however, platelet accumulation is rapid, leading to a large plug that is forced downstream (Figure 7E). Fibrin accumulation under these conditions showed a modest increase with increasing distance downstream (Figure 7F).

Confocal sections (2 μm) were taken of a thrombus formed for 430 seconds on collagen and TF. Figure 8 is a 3-dimensional reconstruction of these images. Cross sections at 25, 75, 125, 175, and 225 μm from the leading edge of the collagen patch were generated to demonstrate the interaction of platelets and fibrin (Figure 8A–8E). As before, platelets (green) were observed forming 30- to 60-μm tall masses at the front of the thrombus (Figure 8A–8C). On the downstream, half of the collagen patch a thick layer of fibrin (≈20 μm) forms punctuated by small platelet mounds that appear slightly taller.

Using COMSOL, the same platelet mass was modeled 3-dimensionally to measure wall shear rate (Figure 8C) and thrombin concentration profiles at a venous inlet shear rate of 200 s^{-1} (Figure 8D). The maximum determined shear rate on the platelet surface reached 4800 s^{-1} whereas most large aggregate peaks were ≈2000 s^{-1} (Figure 8C). The velocity profile resulted in a thrombin boundary layer that diminished to <5% of its maximal value (520 nmol/L) within 20 μm from the platelet surface. This boundary layer thickness agrees precisely with the observed fibrin height downstream of the platelet mass (Figure VI in the online-only Data Supplement).

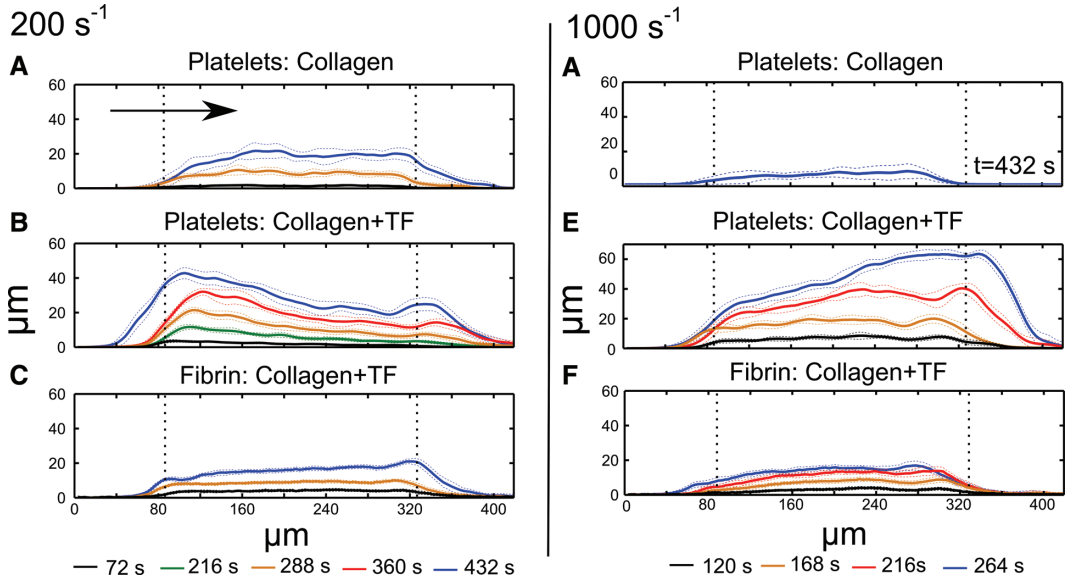

Figure 7. Profiles of platelet aggregate height (the arrow indicates the direction of flow) were generated for whole blood corn trypsin inhibitor (CTI) perfused (200 s^{-1}; constant flow rate) over collagen surfaces (**A**) or collagen surfaces with tissue factor (TF, **B**). The vertical, dashed lines indicate the beginning and end of the collagen strip. The profiles represent the average height (calculated by fluorescent intensity) of 50 lines drawn in the direction of flow for 5 separate clots±SD (dotted lines). Platelets adhering to collagen surfaces (**A**) generate uniform aggregates compared with those formed in the presence of TF (**B**). By supporting thrombin generation platelet deposits become larger and tend to the upstream end of the collagen patch. The polymerization of fibrin is also observed in the presence of TF (**C**), which appears as a mat that becomes thicker downstream, rarely exceeding 20 μm in height. Arterial inlet shear rate conditions (1000 s^{-1}; constant flow rate) were also considered. **D**, In the absence of TF, platelet adhesion to collagen surfaces is diminished compared with venous flow environments. **E**, When TF is present, large platelet masses form rapidly. The large plug is forced downstream as it approaches full occlusion of the channel. Under constant flow rate conditions, these clots would embolize, under pressure relief they would fully occlude the channel. **F**, The morphology of fibrin formation at arterial conditions looks similar to venous conditions.

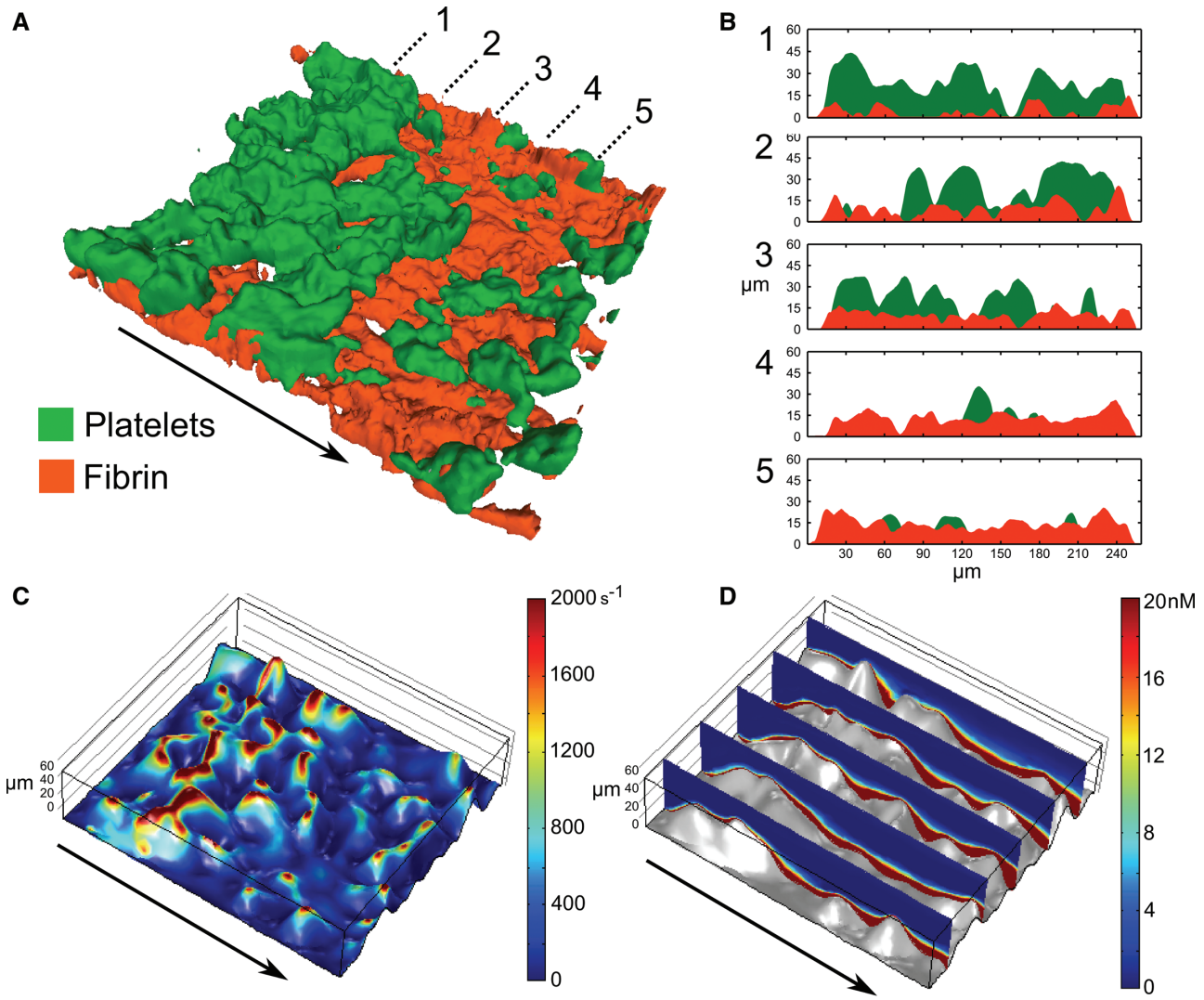

Figure 8. **A**, A 3-dimensional reconstruction of a thrombus formed on collagen and tissue factor immediately after cessation of flow (200 s^{-1}; constant flow rate; 432 seconds). Flow is indicated by the arrow. **B**, Cross sections generated from the confocal images are presented at 25, 75, 125, 175, and 225 μm from the beginning of the collagen patch (1–5, respectively). Fibrin appears within platelet masses, acting as anchors securing them to the surface. Using the surface data, a 3-dimensional model was also generated in COMSOL. Blood flow over the surface was simulated at 2 μL/min, and a thrombin flux of 10 to 12 nmol/μm^2s from the platelet surface was imposed. **C**, Shear rates increased 10-fold from the inlet shear rate (200 s^{-1}) as large platelet aggregates obstructed the channel. **D**, Thrombin boundary layer is indicated in red, where thrombin concentrations exceed 20 nmol/L. The height of this boundary layer was thickest downstream, and did not exceed 20 μm.

Discussion

In the present study, coagulation and platelet aggregation are combined in a single microfluidic model of vessel injury. Through the use of TF-liposomes immobilized on a collagen surface, we demonstrated robust potentiation of platelet aggregation and fibrin production compared with thrombosis on collagen surfaces lacking TF. We manipulated the flow environments within our microfluidic design to study the role that coagulation plays on clot growth and stability under different shear rate conditions. In pressure relief mode, we calculated a biphasic response in shear rate whereas in constant flow rate mode, shear rates monotonically increase during the growth of a thrombus. Through the use of GPRP, we decoupled the production of thrombin and the generation of fibrin and determined, quantitatively, that the fibrin mesh confers a 12- to 28-fold increase in shear resistance on a growing clot. Platelet-fibrin clots withstood ≈2400 dyne/cm^2 whereas clots grown in the presence of GPRP embolized when shear rate conditions reached a maximum of 87 dyne/cm^2. These results agree well with a qualitative report by Wagner et al[14] who performed a flow chamber experiment at arterial shear, but relied on bulk formation of thrombin via the contact pathway in lightly heparinized blood. Furthermore, the assay revealed a 2-fold reduction in fibrin accumulation at arterial inlet shear rates under pressure relief conditions compared with venous inlet shear rate conditions. This result is likely a combination of the decreased time to full occlusion observed under arterial inlet shear rate as well as the decreased residence time at the injury site under the increase in flow rate.

Although platelet deposition and fibrin polymerization occur concurrently in the assay, we observed a spatial distinction in which platelets form large aggregates upstream and fibrin a

thick mat downstream. We confirmed this trend by averaging many line scans from many different thrombi in the direction of flow. The time required for fibrinogen to be cleaved by thrombin and undergo the subsequent polymerization reaction may explain why accumulation is preferred downstream. Confocal imaging revealed that the fibrin mesh formed in the clot was restricted to ≈20 μm in height whereas platelets were able to fully occlude the channels (60 μm). Cross sections of the confocal images suggest that fibrin was present within the platelet aggregates, anchoring them to the collagen surface. The pattern of fibrin formation was also supported by a 3-dimensional COMSOL simulation that calculated steady-state thrombin concentrations assuming a thrombin flux of 10 to 12 nmol/μm^2-s from the platelet surface. The model demonstrated that convective flow thins the thrombin boundary layer over large platelet aggregates upstream whereas a diminished platelet surface height downstream led to a thicker boundary layer. Notably, the downstream thrombin boundary layer reached heights of ≈20 μm above the collagen surface before thrombin concentrations diminished to <5% of their maximal value. Coupling these transport properties with the number of events required for the transition from fibrinogen to fibrin polymer helps elucidate the preference for fibrin mesh accumulation downstream of the large platelet aggregates.

The intersection of fibrin generation and platelet recruitment at sites of vascular injury is an important topic in a variety of pathophysiological conditions. In hemophilia, for example, defects in thrombin production affect platelet activation,[24] fibrin generation,[25] and clot stabilization.[26,27] The relative roles that these deficiencies play in the bleeding complications are not well understood, but have implications regarding initiation and growth of a stable thrombus as well as its lytic susceptibility.[28] We have attempted to recreate the conditions of severe hemophilia in our microfluidic model through the use of neutralizing antibodies against FIX and hemophilia A plasma with high titers of antibodies against FVIII (Materials and Methods in the online-only Data Supplement). We have demonstrated that this cocktail is effective at slowing coagulation triggered by dilute TF (1 pmol/L–500 fmol/L) up to 2-fold in a fluorogenic assay with a thrombin-sensitive substrate (Figure VIIA in the online-only Data Supplement) but not at higher concentrations (10-pmol/L TF). Under flow conditions on TF/collagen surfaces, normal donor blood treated with the same neutralizing antibodies showed no significant decrease in platelet or fibrin deposition (data not shown), suggesting that the formation of the extrinsic tenase is dominant. Because the intrinsic tenase is important during the propagation phase of coagulation,[29] we attempted to slow the formation of the in vitro clot by adding the antiplatelet agent iloprost (1 nmol/L). Iloprost (Figure VIIB in the online-only Data Supplement) revealed a subtle but significant ($P<0.01$; n=5 experiments; 20 clotting events per condition) reduction in platelet accumulation (17±3%) and a significant ($P<0.05$) reduction in fibrin deposition of 23±17%. Under these conditions, platelet and fibrin accumulation was compared by donor, because interdonor variation would have masked the effects of neutralizing intrinsic tenase. Our findings suggest that the extrinsic tenase can substitute for the intrinsic tenase at injury sites with sufficiently high TF. The observation that hemophiliacs often bleed into their joints, an area thought to have low quantities of TF[30] suggests that the intrinsic tenase may be necessary under these conditions. Therefore we attempted to neutralize the intrinsic tenase in the presence of 1:9 diluted TF under venous flow conditions. These conditions revealed a decrease in platelet fluorescent intensity of 30±13%, but fibrin generation was too low to demonstrate an effect due to blocking FIXa/FVIIIa (Figure VIIC in the online-only Data Supplement).

The present study represents a new technique to study the role of coagulation in clot growth and stability in a physiologically relevant environment. The formation of fibrin networks and the resulting strength of the clots have been studied extensively, but we are not aware of any reports that combine this with whole blood under flow. In earlier work, our group has shown that morphology of fibrin polymerization, using purified proteins under flow, was dependent on shear rate (10–100 s^{-1}) as well as the flux of thrombin introduced to the flow.[31] In silico, Guy et al[4] have predicted that the growth of a fibrin gel is dependent on shear (0–1000 s^{-1}), thrombin generation/inhibition, and gel permeability. Models like these highlight the complexity of the in vivo injury site by combining the intricate mechanisms of protein transport around the thrombus, a feature that is inherent to our assay.

Conclusion

Using patterned microfluidic surfaces which incorporate important triggers for coagulation (TF) and for platelet aggregation (collagen), we have investigated the effects of fibrin mesh formation on thrombus growth, stability, and embolization. We report that the fibrin network confers a 12- to 28-fold increase in shear resistance to the growing clot, allowing it to resist shear stress in excess of 2000 dyne/cm^2.

Acknowledgments

We thank Dr Mortimer Poncz for providing the fibrin-specific antibody (T2G1).

Sources of Funding

This work was supported by the National Institutes of Health grant (NIH R01 HL103419) to Dr Diamond and a predoctoral training grant (5T32HL007439-33) to T. Colace from the NIH.

Disclosures

None.

References

1. Hathcock JJ, Nemerson Y. Platelet deposition inhibits tissue factor activity: *in vitro* clots are impermeable to factor Xa. *Blood*. 2004;104:123–127.
2. Kuharsky AL, Fogelson AL. Surface-mediated control of blood coagulation: the role of binding site densities and platelet deposition. *Biophys J*. 2001;80:1050–1074.
3. Leiderman K, Fogelson AL. Grow with the flow: a spatial-temporal model of platelet deposition and blood coagulation under flow. *Math Med Biol*. 2011;28:47–84.
4. Guy RD, Fogelson AL, Keener JP. Fibrin gel formation in a shear flow. *Math Med Biol*. 2007;24:111–130.
5. Okorie UM, Denney WS, Chatterjee MS, Neeves KB, Diamond SL. Determination of surface tissue factor thresholds that trigger coagulation at venous and arterial shear rates: amplification of 100 fM circulating tissue factor requires flow. *Blood*. 2008;111:3507–3513.

6. Chatterjee MS, Denney WS, Jing H, Diamond SL. Systems biology of coagulation initiation: kinetics of thrombin generation in resting and activated human blood. *PLoS Comput Biol*. 2010;6:pii: e1000950.
7. Schneider SW, Nuschele S, Wixforth A, Gorzelanny C, Alexander-Katz A, Netz RR, Schneider MF. Shear-induced unfolding triggers adhesion of von Willebrand factor fibers. *Proc Natl Acad Sci USA*. 2007;104: 7899–7903.
8. Shankaran H, Alexandridis P, Neelamegham S. Aspects of hydrodynamic shear regulating shear-induced platelet activation and self-association of von Willebrand factor in suspension. *Blood*. 2003;101:2637–2645.
9. Berny MA, Munnix IC, Auger JM, Schols SE, Cosemans JM, Panizzi P, Bock PE, Watson SP, McCarty OJ, Heemskerk JW. Spatial distribution of factor Xa, thrombin, and fibrin(ogen) on thrombi at venous shear. *PLoS ONE*. 2010;5:e10415.
10. Dubois C, Panicot-Dubois L, Merrill-Skoloff G, Furie B, Furie BC. Glycoprotein VI-dependent and -independent pathways of thrombus formation in vivo. *Blood*. 2006;107:3902–3906.
11. Colace TV, Jobson J, Diamond SL. Relipidated tissue factor linked to collagen surfaces potentiates platelet adhesion and fibrin formation in a microfluidic model of vessel injury. *Bioconjug Chem*. 2011;22:2104–2109.
12. Shen F, Kastrup CJ, Liu Y, Ismagilov RF. Threshold response of initiation of blood coagulation by tissue factor in patterned microfluidic capillaries is controlled by shear rate. *Arterioscler Thromb Vasc Biol*. 2008;28:2035–2041.
13. Kastrup CJ, Shen F, Runyon MK, Ismagilov RF. Characterization of the threshold response of initiation of blood clotting to stimulus patch size. *Biophys J*. 2007;93:2969–2977.
14. Wagner WR, Hubbell JA. Local thrombin synthesis and fibrin formation in an *in vitro* thrombosis model result in platelet recruitment and thrombus stabilization on collagen in heparinized blood. *J Lab Clin Med*. 1990;116:636–650.
15. Falati S, Gross P, Merrill-Skoloff G, Furie BC, Furie B. Real-time *in vivo* imaging of platelets, tissue factor and fibrin during arterial thrombus formation in the mouse. *Nat Med*. 2002;8:1175–1181.
16. Furie B, Furie BC. Thrombus formation in vivo. *J Clin Invest*. 2005;115:3355–3362.
17. Kudryk B, Rohoza A, Ahadi M, Chin J, Wiebe ME. Specificity of a monoclonal antibody for the NH2-terminal region of fibrin. *Mol Immunol*. 1984;21:89–94.
18. Litvinov RI, Gorkun OV, Galanakis DK, Yakovlev S, Medved L, Shuman H, Weisel JW. Polymerization of fibrin: direct observation and quantification of individual B:b knob-hole interactions. *Blood*. 2007;109:130–138.
19. Smith SA, Morrissey JH. Rapid and efficient incorporation of tissue factor into liposomes. *J Thromb Haemost*. 2004;2:1155–1162.
20. Maloney SF, Brass LF, Diamond SL. P2Y12 or P2Y1 inhibitors reduce platelet deposition in a microfluidic model of thrombosis while apyrase lacks efficacy under flow conditions. *Integr Biol (Camb)*. 2010;2:183–192.
21. Folie BJ, McIntire LV. Mathematical analysis of mural thrombogenesis. Concentration profiles of platelet-activating agents and effects of viscous shear flow. *Biophys J*. 1989;56:1121–1141.
22. Neeves KB, Maloney SF, Fong KP, Schmaier AA, Kahn ML, Brass LF, Diamond SL. Microfluidic focal thrombosis model for measuring murine platelet deposition and stability: PAR4 signaling enhances shear-resistance of platelet aggregates. *J Thromb Haemost*. 2008;6:2193–2201.
23. Hubbell JA, McIntire LV. Technique for visualization and analysis of mural thrombogenesis. *Rev Sci Instrum*. 1986; 57:892–897.
24. Aljamali MN, Kjalke M, Hedner U, Ezban M, Tranholm M. Thrombin generation and platelet activation induced by rFVIIa (NovoSeven) and NN1731 in a reconstituted cell-based model mimicking haemophilia conditions. *Haemophilia*. 2009;15:1318–1326.
25. Brummel-Ziedins KE, Branda RF, Butenas S, Mann KG. Discordant fibrin formation in hemophilia. *J Thromb Haemost*. 2009;7:825–832.
26. Wolberg AS, Allen GA, Monroe DM, Hedner U, Roberts HR, Hoffman M. High dose factor VIIa improves clot structure and stability in a model of haemophilia B. *Br J Haematol*. 2005;131:645–655.
27. Dargaud Y, Prevost C, Lienhart A, Claude Bordet J, Negrier C. Evaluation of the overall haemostatic effect of recombinant factor VIIa by measuring thrombin generation and stability of fibrin clots. *Haemophilia*. 2011;17:957–961.
28. Wolberg AS, Campbell RA. Thrombin generation, fibrin clot formation and hemostasis. *Transfus Apher Sci*. 2008;38:15–23.
29. Hockin MF, Jones KC, Everse SJ, Mann KG. A model for the stoichiometric regulation of blood coagulation. *J Biol Chem*. 2002;277:18322–18333.
30. Drake TA, Morrissey JH, Edgington TS. Selective cellular expression of tissue factor in human tissues. Implications for disorders of hemostasis and thrombosis. *Am J Pathol*. 1989;134:1087–1097.
31. Neeves KB, Illing DA, Diamond SL. Thrombin flux and wall shear rate regulate fibrin fiber deposition state during polymerization under flow. *Biophys J*. 2010;98:1344–1352.